

Development of New Pole Figure Method for Directly Projecting Grains with High Speed and High Resolution Using Synchrotron Radiation, and Its Application for Observing Electrical Steel and Mild Steel Sheets at High Temperatures

Koichi Kawasaki*¹
Takahide Shimazu*³
Yasuharu Sakuma*³

Hiroshi Iwasaki*²
Naoki Yoshinaga*³
Toshiharu Kikuchi*³

Abstract:

A new pole figure method was developed for projecting individual grains with high speed and resolution by taking advantage of the extreme brilliance of synchrotron radiation and the high sensitivity of imaging plates. Previously considered unfeasible, this is a "direct pole figure method" that has expanded the scope of the traditional point-by-point pole figure method for application to dynamic and local analyses. An X-ray heating furnace was also developed, and at the Photon Factory of the National Laboratory for High Energy Physics it was used to observe the explosive growth of Goss-oriented grains in the secondary recrystallization process of electrical steel sheets at high temperatures. Using the new pole figure method it was possible to measure the high-temperature texture in the austenitic region of mild steel sheets and locate the formation mechanism of the transformation texture. It was also possible to detect the change in the pole figures of aluminum alloys between rolling and recrystallization, and observe their primary recrystallization process. The new pole figure method is expected to have applications in studying the recrystallization and measuring pole figures of microregions and coarse grains at high temperatures.

1. Introduction

Various materials are used in today's industrial technology society, and many of them are metals and alloys. These materials are mostly available in plate, sheet, wire and bar forms. They are also fabricated into complex shapes. All of these materials are

polycrystalline. Grain orientations depend on the type of manufacturing process. A plate or sheet material starts as an ingot and undergoes repeated rolling and heating until the required thickness is reached. As the material is processed through these steps, its grain orientation distribution assumes a rolling texture or a recryst-

*1 Technical Development Bureau (presently Niihama National College of Technology)

*2 National Laboratory for High Energy Physics (presently Ritsumeikan University)
*3 Technical Development Bureau

tallization texture. The fabrication, magnetic, electric, and other properties of the material are greatly affected by its grain orientation distribution. The specific manufacturing processes involved are designed to achieve a desired grain orientation distribution.

The pole figure method is used to show the grain orientation distribution of materials. Its principle is described in detail in reference 1). Simply speaking, the positions of poles of normals to a given atomic plane of a grain, for example, the $\{111\}$ plane of a face-centered cubic lattice, are shown on the surface of a sphere of poles. Fig. 1 is the $\{111\}$ pole figures of a rolled aluminum sheet obtained by the conventional point-by-point method²⁾. In Fig. 1, RD refers to the rolling direction of the sheet, and TD is the transverse direction of the sheet. The direction perpendicular to the page is the normal direction (ND) of the sheet. X-ray diffractometry is the general method for experimentally determining such a pole figure³⁾. The sample is placed at the center of the diffractometer, the X-ray scintillation counter is fixed at an angle where the Bragg reflections from a given atomic plane can be observed, and the intensity of the Bragg reflections are measured while changing the azimuth and pole angle of the sample by using the sample rotating mechanism of the diffractometer. The intensity values are recorded on the surface of the sphere of the poles, and their distribution is presented by contour lines. This measuring method is known as the point-by-point method and it takes about one hour to complete a pole figure by using an ordinary X-ray source. To observe the azimuth and pole angle grain orientation distribution decomposed in detail, an entire day is required.

In the area of material research, there is a need for elucidating the mechanism of change in material properties by tracking the way the grain orientation distribution rapidly changes under the influence of heat, for example. This cannot be accomplished with the point-by-point method using a laboratory X-ray source, however. The authors have been carrying out X-ray diffraction research by using the extreme brilliance of synchrotron radiation. A method was developed for dynamically observing the change in the grain orientation distribution of materials by adopting a highly sensitive, two-dimensional detector. It was successfully applied to the observation of the secondary recrystallization process in elec-

trical steel at high temperatures³⁾. This report will first explain the pole figure measuring method by introducing an example of an aluminum alloy, and then describe the results of applications, including those with steel sheets. The possibility of the new pole figure method enabling uses in other applications will be discussed last.

2. Principle of High-Speed and High-Resolution Pole Figure Method

The principle of the high-speed and high-resolution pole figure method developed by the authors is illustrated in Fig. 2³⁾. The atomic plane corresponding to poles of normals on the line of intersection between the sphere of poles and the Ewald sphere causes Bragg reflections. Bragg reflections are projected and recorded as circular arcs on the imaging plate⁴⁾, which is placed on the upper right side. The imaging plate is a new type of two-dimensional detector with a high detection sensitivity⁴⁾. At this time, Bragg reflections are also produced from atomic planes not to be measured. The screen with an arc-shaped slot is placed in front of the detector to remove these Bragg reflections. In this arrangement, the Ewald sphere (actually the sample) is rotated to move the line of intersection with the sphere of poles. When the imaging plate is moved parallel in synchrony with this rotary movement, the intensity distribution on the sphere of poles is recorded on the imaging plate. Naturally, the transfer of the distribution from the three-dimensional sphere to the two-dimensional plate introduces distortion in the shape of the pole figure. The pole figure also varies in the magnitude of scale in the scanning direction, depending on the magnitude of the rotating speed. These factors, however, do not introduce any intrinsic difficulty into the interpretation of the measured results. If necessary, the measured results can be geometrically corrected to obtain a distortion-free pole figure.

Fig. 3(a) shows the transmitted pole figure (partial) of a cold-rolled aluminum alloy sheet recorded by the new pole figure method using monochromatized synchrotron radiation (wavelength of 0.06 nm) as an incident beam and an imaging plate. The rotational angle range of the Ewald sphere is 40°. The region

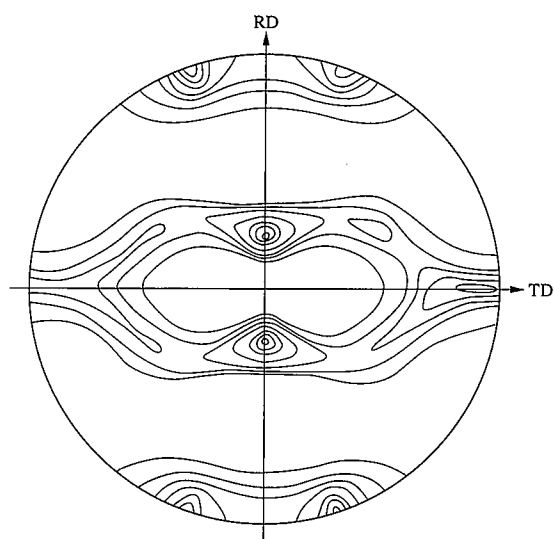


Fig. 1 $\{111\}$ pole figure of cold-rolled aluminum sheet measured by point-by-point method²⁾

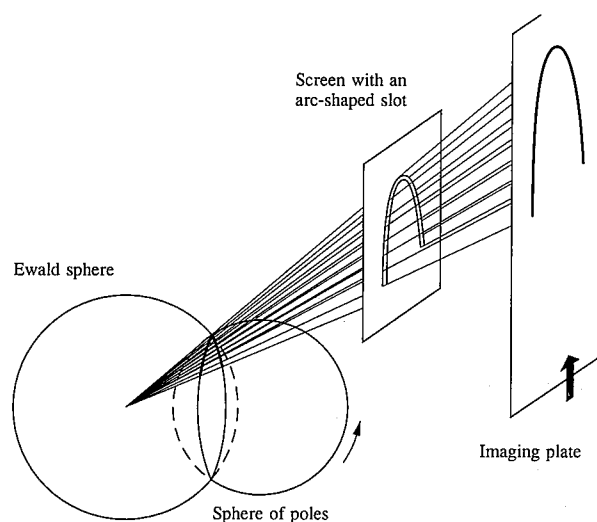


Fig. 2 Principle of high-speed and high-resolution pole figure method

scanned in this measurement is shown in **Fig. 3(b)** as indicated by the broken line in the partial pole figure of **Fig. 1**. Since the aluminum alloy is low in the alloy content, the pole figure measured by the new pole figure method (shown in **Fig. 3(a)**) is almost the same as that measured by the conventional point-by-point method (shown in **Fig. 3(b)**). The two orientation distribution peaks near the north pole and the blank space just below are clearly recorded. The fan-shaped region that indicates the scanning region of **Fig. 3(b)** increases in width at the top and bottom when the rotational angle range of the Ewald sphere is increased and expands in area when the length of the arc-shaped slot is increased. The time required to obtain the pattern of **Fig. 3(a)** was a short 80 seconds, attesting to the extreme brightness of synchrotron radiation. As another example, **Photo 1** shows the pole figure (partial) of a recrystallized aluminum alloy sheet measured by the new pole figure method at room temperature. The same region as shown in **Fig. 3** was scanned. It is evident that recrystallization at about 800 K drastically changed the texture and moved the orientation distribution peaks to the blank region in **Fig. 3 (a)**. It should be noted here that the reflections from individual grains are recorded without decomposition in **Fig. 3(a)**, but that grain growth due to recrystallization is plainly depicted in **Photo 1**. If the two samples are measured by the point-by-point method and their grain orientation distributions can be represented by contour lines, the only difference between them will be the movement of the orientation distribution peaks. The cold-rolled aluminum alloy sheet has a small grain size and exhibits rolling strain immediately after the rolling operation. When measured by the new pole figure method, the pole figure of the sheet in the as-cold-rolled con-

dition reveals a continuous dark and white pattern. When the sheet is recrystallized, the grains grow and the rolling strain dissipates. When measured by the new pole figure method, the pole figure of the sheet in the recrystallized condition shows that the continuous dark and white pattern has changed to a spot pattern. This is due to the high spatial and angular resolution of the new pole figure method, which can more accurately reveal the state of materials than the conventional point-by-point method.

A literature search revealed that the idea of a two-dimensional recording of a pole figure as depicted in **Fig. 2** was proposed by Guinier⁹ and others around 1950. It took a long time to obtain a single pattern when an ordinary X-ray source and film were used. For this reason, the idea found no practical application and has been buried in obscurity.

If a pole figure (partial) of a material is recorded in a matter of minutes by using synchrotron radiation, the change in the grain orientation distribution of the material can be tracked in real time. That is, the distribution of poles in the same angular range on the sphere of poles can be continuously recorded by repeating the rotary movement of the Ewald sphere (actually of the sample) and continuously moving the long two-dimensional detector in one direction as shown in **Fig. 2**. This is the high-speed and high-resolution pole figure method developed by the authors to dynamically observe grain orientation distribution. The method's actual experimental arrangement will be described in the next chapter.

3. Experimental Procedure

The apparatus for the high-speed and high-resolution pole figure method is schematically illustrated in **Fig. 4**. A high-tempera-

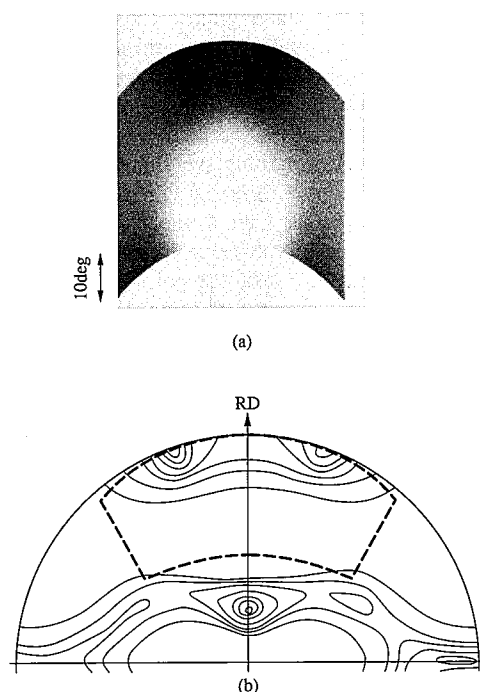


Fig. 3 (a) $\{111\}$ pole figure (partial) of 1-mm thick cold-rolled aluminum sheet measured by new method at room temperature. Sample rotation angle range: 40° , projection time: 80 seconds
(b) Scan region of (a)

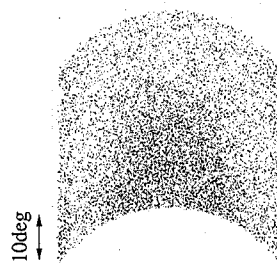


Photo 1 $\{111\}$ pole figure (partial) of 1-mm thick recrystallized aluminum alloy sheet measured by new method

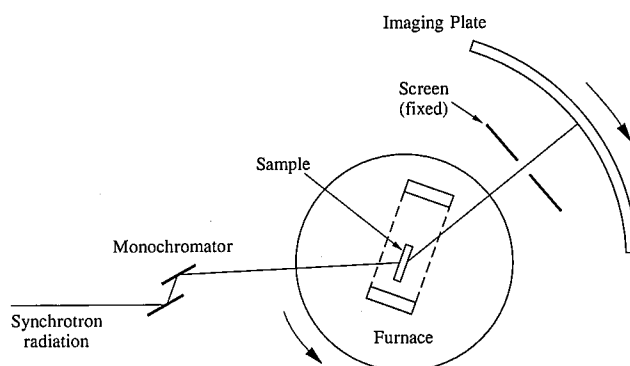


Fig. 4 Schematic illustration of system for high-speed and high-resolution pole figure method

ture heating furnace was mounted in the sample stage of the four-circle X-ray diffractometer⁶⁾. This was installed in the beam line BL-3A⁷⁾ of the 2.5 GeV ring, which was located at the National Laboratory for High Energy Physics' Photon Factory. The sample was placed in the heating furnace, which in turn was rotated by using the ϕ -axis mechanism of the diffractometer. At the same time, the two-dimensional detector was moved by using the 2θ -axis rotation mechanism of the diffractometer.

The high-temperature heating furnace was developed to dynamically observe electrical steel sheets under the same environment as when they are heat treated. The electrical steel sheet sample measured 0.2 mm thick, 70 mm long, and 10 mm wide. The sample temperature was measured with a thermocouple. The sample temperature variations during holding were held within ± 1 K at 1,233 K with respect to the target temperature as obtained by the PID control method. The sample temperature uniformity was within ± 5 K over an area of 5 by 5 mm at 1,233 K. To examine the effect of tensile strain on secondary recrystallization, the mechanism for applying tensile strain to the sample was added to the heating furnace. Provision was also made for flowing argon gas to keep the furnace under a neutral atmosphere during heating.

Photo 2 is a photograph of the measuring system. Shown at the center is the heating furnace mounted in the diffractometer. The screen with an arch-shaped slot and the curved holder to which the imaging plate is attached are also noticeable. The distance from the sample to the screen is 200 mm, and the distance from the sample to the detector is 310 mm. The imaging plate used here as a detector is 200 mm wide and 400 mm long.

The BL-3A is a beam line that utilizes synchrotron radiation from a bending magnet. A pair of silicon single crystals (the (111) plane being the reflecting plane) comprises the monochromator⁷⁾. The beam of synchrotron radiation irradiates the sample in the heating furnace. Diffracted X-rays pass the furnace window material, heater plate, and insulating plate. The shorter the wavelength of synchrotron radiation used, the smaller the amount of synchrotron radiation absorbed by these materials. Synchrotron radiation weakens in spectral intensity at the low end of the wavelength range. The angular position where a wide-area two-dimensional detector can be installed in the diffractometer is limited.

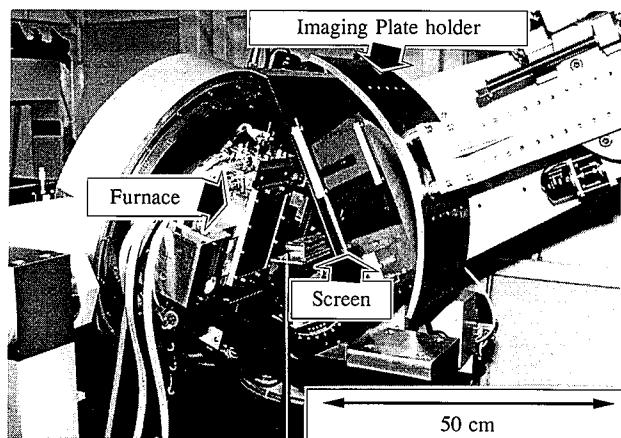


Photo 2 System for high-speed and high-resolution pole figure method installed at Photon Factory, National Laboratory for High Energy Physics

Given these factors, 0.06 nm was selected as the optimum wavelength. A notable characteristic of synchrotron radiation is the freedom with which the wavelength can be selected, making it extremely easy to establish experimental conditions. The total amount of absorption at this wavelength by the sample, window material, heater plate, and so on is 4.0 μ t.

The average current of the light source ring in the experiment was 300 mA. The sample in the BL-3A beam line is located at 28 m from the light source. The second crystal in the monochromator was curved to focus the monochromatized incident beam within a horizontal plane. The beam incident on the sample measured 4 mm long and 4 mm wide.

4. Application to Observation of Secondary Recrystallization Process of Electrical Steel Sheets at High Temperatures

4.1 Secondary recrystallization of electrical steel sheets

It is vital to reduce the core loss or energy loss of electrical steel sheets (iron-silicon alloy sheets) used in large quantities in transformers, motors, and other electrical machinery. Annual electrical steel sheet consumption is approximately 1,000,000 tons in Japan. The resultant core loss per year amounts to an enormous ¥1 trillion or so in terms of electric power costs. Cutting down this core loss is an urgent and important energy conservation issue. Transformer material containing 3% by weight of silicon is melted, and rolled and heated several times before it becomes a finished product. When the rolled sheet is heated for a short time (about one minute), primary recrystallization occurs and results in a uniform structure of fine grains of about 20 μ m in diameter (primary recrystallization structure). In this state, the sheet still exhibits large core loss. High-temperature heating causes an important microstructural change, called secondary recrystallization, producing huge grains. The secondary recrystallization structure is composed of huge grains measuring 2 to 10 mm in diameter and markedly lower in the core loss.

The room-temperature $\{100\}$ pole figures of an electrical steel sheet sample measured by the point-by-point method before and after high-temperature heating are shown in **Figs. 5(a)** and **5(b)**, respectively. The pole figure of **Fig. 5(b)** was constructed from the data obtained by the Laue method⁸⁾. The crystal structure of the Fe-3%Si alloy is a body-centered cubic lattice structure. **Fig. 5** shows the distribution of the poles normal to its $\{100\}$ plane. **Fig. 5(a)** shows the pole figure of the sample before high-temperature heating in which mild orientation peaks are observed in the vicinity of the north and south poles. Secondary recrystallization produced sharp orientation peaks at two positions on the equator in addition to those at the north and south poles as shown in **Fig. 5(b)**. The orientation distribution of **Fig. 5(b)** shows that the $\{110\}$ plane and $\langle 001 \rangle$ direction of the grains are parallel to the rolling plane and direction of the sheet, respectively. Since the easy magnetization axis of the alloy is the $\langle 001 \rangle$ direction, the core loss in the rolling direction is reduced as a result. This grain orientation is called the Goss orientation after the name of the inventor⁹⁾ and written as the $\{110\}\langle 001 \rangle$ orientation. A key point in the electrical steel manufacturing process is the amount of the Goss-oriented grains produced. In actual materials, it is rare that the $\{110\}$ plane and the $\langle 001 \rangle$ direction become completely parallel with the sheet surface and the rolling direction, respectively. If grain orientations fall within 7° from the ideal orientation, for example, they are defined as Goss orientations.

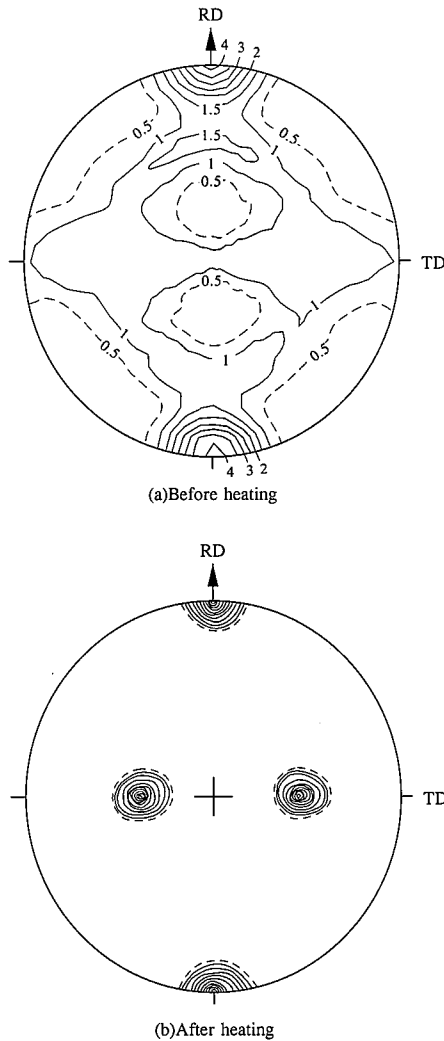


Fig. 5 Room-temperature $\{100\}$ pole figures of electrical steel sheet measured by point-by-point method before high-temperature heating (a) and after high-temperature heating (b). Constructed from data obtained by Laue method⁹⁾

No attempts have been made yet to observe under real environmental and time conditions the mechanisms whereby the electrical steel grains change in orientation and grow during high-temperature heating for secondary recrystallization. MacCormack and Tanner¹⁰⁾ observed electrical steel sheet samples at high temperatures in the primary recrystallization process by synchrotron radiation topography. Since they used X-ray films, they could not obtain satisfactory results. Therefore the secondary recrystallization process of electrical steel sheets at high temperatures was left unsolved.

4.2 Dynamic observation of secondary recrystallization process

When following the change in the grain orientation distribution of electrical steel sheet samples during secondary recrystallization, an important portion from the pole figure of the sample was selected and the measuring attention at that portion was focused by considering the fact that the entire process would be completed in about 10 min. The pole figure of Fig. 5(a) is reproduced in Fig. 6, where the measured region is shaded. The first measurement series tracked the change in the orientation distribu-

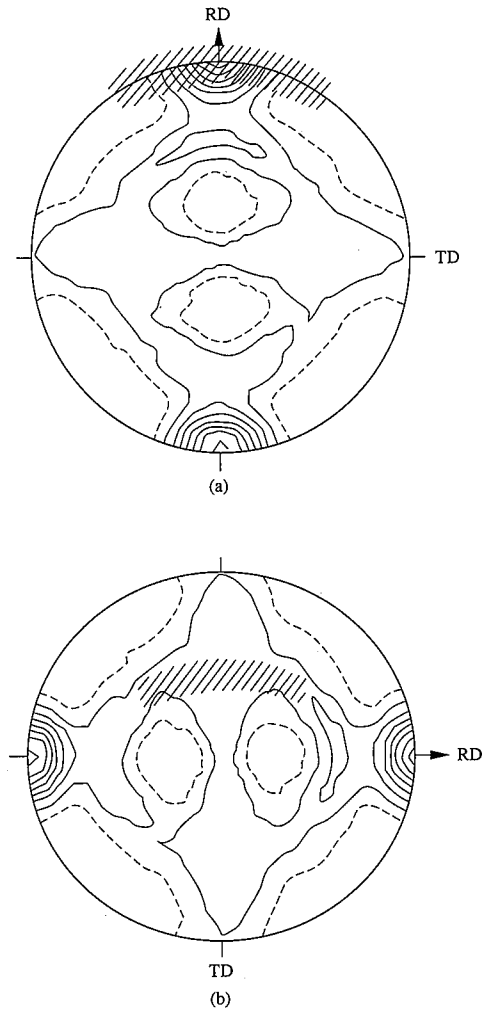


Fig. 6 Regions of high-temperature pole figure of electrical steel sheet measured by new method. Fig. 5(a) is reproduced here, and measured regions are shaded. (a) Region near north pole, (b) region near equator

tion near the north pole as shown in Fig. 6(a), while the second measurement series tracked the change in the orientation distribution near the equator as shown in Fig. 6(b). The sample was machined in the transverse direction (TD) in Fig. 6(a) and in the rolling direction (RD) in Fig. 6(b). The rotational angle range of the Ewald sphere required to scan the shaded region was 10° . The sample was set in the heating furnace, heated at a rate of 1 K per second, isothermally held at 1,233 K, and immediately measured. The results obtained are shown in Photo 3. The change in the pole figure near the north pole is depicted. The intensity of the Bragg reflections at the higher temperature markedly decreases compared with those at room temperature. The time required to record one pattern within the rotational angle range of 10° was still 40 seconds. The time elapsed after the start of high-temperature holding is indicated as zero seconds and so on along the right side. When one scan was completed, 80 seconds were required to return the sample to the original angular position and to scan the sample again. This means that the sample was scanned for the second time 120 seconds after the start of heating. The pattern recorded immediately after heating or the bottom pattern shows

the grain orientation distribution that corresponds to the pole figure of Fig. 6(a) recorded before heating. In other words, heating does not immediately change the grain orientation distribution. This is also true of the pattern recorded 120 seconds later. At 240 seconds, a sudden and severe grain orientation distribution concentration occurred, and a sharp peak formed. The peak increased in integrated intensity with the elapse of time (This will be described later). The pole figure changes continuously measured near the equator are shown in Photo 4. The first pattern also corresponds to the pole figure of Fig. 6(b) before high-temperature heating. In this case, the distribution reveals no concentration of grain orientations. An explosively sharp peak also appeared at 240 seconds after the start of isothermal holding. The peaks shown in Photo 3 and Photo 4 correspond to those shown in Fig. 5(b) and resulted from the Goss-oriented grains. As discussed previously, there is a period of time during which no change appears to occur in the initial stage of the secondary recrystallization process of electrical steel sheets. This is called the incubation period here. The presence of the incubation period and the explosive grain growth thereafter were confirmed for the first time by the dynamic observations reported here.

Next, the effect of strain on the secondary recrystallization process was examined. The straining of the sample was started at 973 K on heating and continued for 300 seconds before the sample was heated to 1,233 K. The sample chucks were moved at a speed of 1 $\mu\text{m/s}$, which translated to a strain rate of the order of $10^{-6}/\text{s}$. Tension was applied to the sample in the rolling direction (RD), the transverse direction (TD), and a third direction falling between the RD and TD. The results did not differ between the three directions. Photo 5 shows the continuously measured grain orientation distributions of a sample subjected to tensile strain. This is a pole figure region near the equator. It should be noted that the explosive appearance of the grain orientation distribution peak is inhibited during the application of tensile strain. As soon as the application of tensile strain is discontinued, the grain orientation distribution peak appears. A similar phenomenon was observed near the north pole as well. These results show that the driving force for the growth of Goss-oriented grains is offset by the presence of tensile strain.

Fig. 7 shows the change in the integrated peak intensity of Goss-oriented grains with the elapse of the isothermal holding time. The peak increases in the integrated intensity with the elapse of the isothermal holding time. This clearly shows the explosive growth of Goss-oriented grains after the incubation period. The prolongation of the incubation period by the tensile strain is also exhibited distinctly. The integrated intensity corresponds to grain volume. The conversion between the two will be discussed in another paper.

The incubation period was discovered in the secondary recrystallization process. A detailed observation was made to investigate the microstructural properties of the incubation period. A sample chemically polished from one side to a thickness of 0.10 to 0.12 mm was used to improve the signal to noise (S/N) ratio. It was confirmed that the sample produced the same secondary recrystallization as observed in a 0.20-mm thick sample. Photo 6 shows patterns near the north pole magnified eight times. Many diffraction spots recorded on the imaging plates can be plainly distinguished. The spots are elongated horizontally because the diffraction beam diverged horizontally. The holding times in Photo 6 range from zero to 360 seconds. The patterns

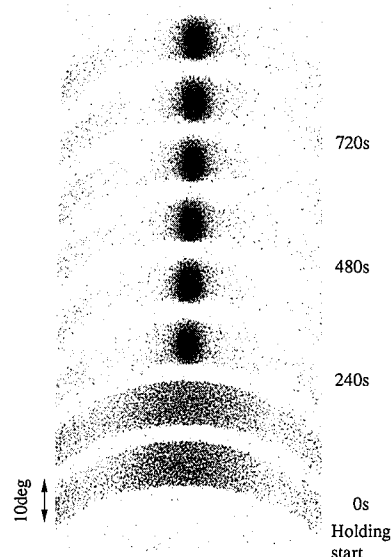


Photo 3 {100} pole figures (partial) of electrical steel sheet repeatedly measured by new method during isothermal holding at 1,233 K. Near north pole, sample rotation angle range: 10° , projection time: 40 seconds, measuring interval: 120 seconds. Explosive growth of Goss-oriented grains after incubation period is shown

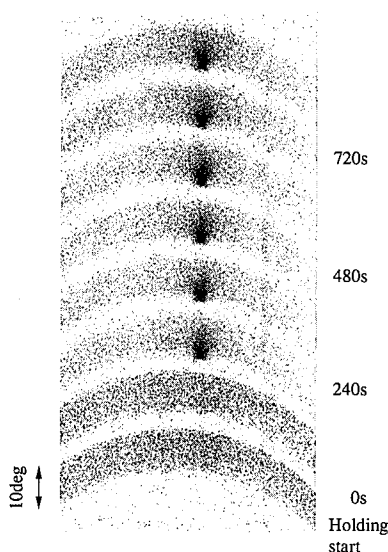


Photo 4 {100} pole figures (partial) of electrical steel sheet repeatedly measured by new method during isothermal holding at 1,233 K. Near equator, sample rotation angle range: 10° , projection time: 40 seconds, measuring interval: 120 seconds. Explosive growth of Goss-oriented grains after incubation period is shown

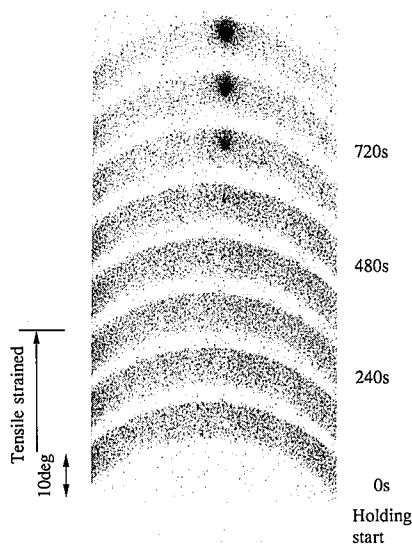


Photo 5 {100} pole figures (partial) of electrical steel sheet under tensile strain repeatedly measured by new method during isothermal holding at 1,233 K. Near equator, sample rotation angle range: 10° , projection time: 40 seconds, measuring interval: 120 seconds. Tensile strain was applied at 973 K on heating and continued for 300 seconds after reaching 1,233 K. Sample chuck speed was $1 \mu\text{m/s}$, and chuck distance was 70 mm. Rapid appearance of Goss-oriented grain peak is suppressed during application of tensile strain

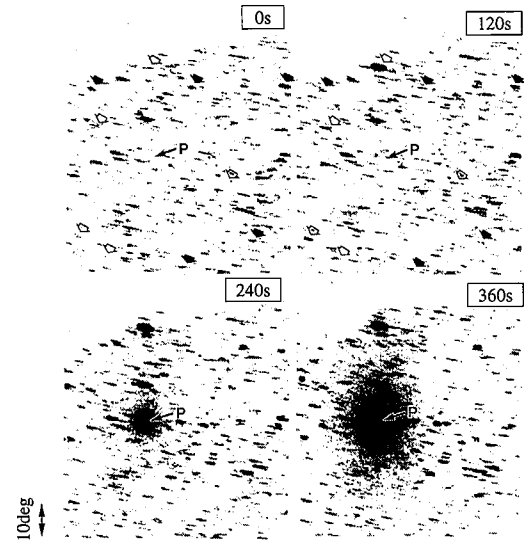


Photo 6 Enlarged view of {100} pole figures (partial) of electrical steel sheet repeatedly measured by new method during isothermal holding at 1,233 K. Projection near north pole is magnified by 8 times, Sample rotation angle range: 10° , projection time: 40 seconds, measuring interval: 120 seconds. P indicates position where Goss-oriented grains grew rapidly. Zero, 120, 240, and 360 seconds are holding time. Large and dark spots are indicated by open arrows, and smaller and less dark spots are indicated by solid arrows

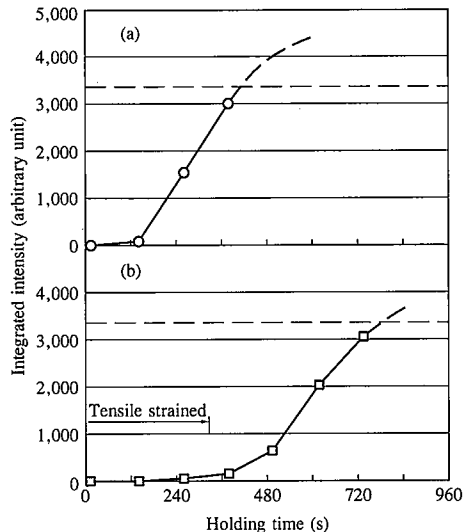


Fig. 7 Change in peak integrated intensity of Goss-oriented grains in electrical steel sheet with elapse of isothermal holding time: (a) without tensile strain as shown in **Photo 4** and (b) with tensile strain as shown in **Photo 5**. Upper broken lines indicate grain growth beyond field of view. Horizontal broken lines indicate integrated intensity corresponding to upper limit of field of view

recorded at zero and 120 seconds appear the same, but a closer examination of the corresponding spots shows that some spots are large and high in the gray level (as indicated by open arrows) and that some spots are smaller and lower in the gray level (as indicated by closed arrows). This situation may be taken to mean that the individual grains have changed in size. In other words, no changes that affect the entire material have occurred during the incubation period, but a "fluctuation" has occurred in the size of the grains (average size of $20 \mu\text{m}$) that compose the material. An orientation distribution peak of Goss-oriented grains appeared at the center of the pattern recorded at 240 seconds in **Photo 6** and had rapidly grown in the pattern recorded at 360 seconds. At the position P where the Goss-oriented grains evolved, spots greater than the average size are not recognized in the patterns recorded at 120 and zero seconds. This fact is significant. That is, when the Goss-oriented grains rapidly grow during secondary recrystallization, large grains to serve as nuclei for the Goss-oriented grains do not exist (or do not appear to exist) in the patterns recorded at time intervals of 120 seconds. This finding gives a hint about the elucidation of the mechanism of the growth of the Goss-oriented grains. Another series of experiments will be conducted at shorter measuring time intervals.

Dynamic topographic observations with synchrotron radiation were also performed to supplement the above-mentioned dynamic observations of the change in the grain orientation distribution. The details are reported in References 11) and 12).

5. Measurement of High-Temperature Pole Figures in Mild Steel Sheets

The high-speed and high-resolution pole figure method allows easy measurement of such high-temperature pole figures. This was previously not possible. The texture at high-temperature was

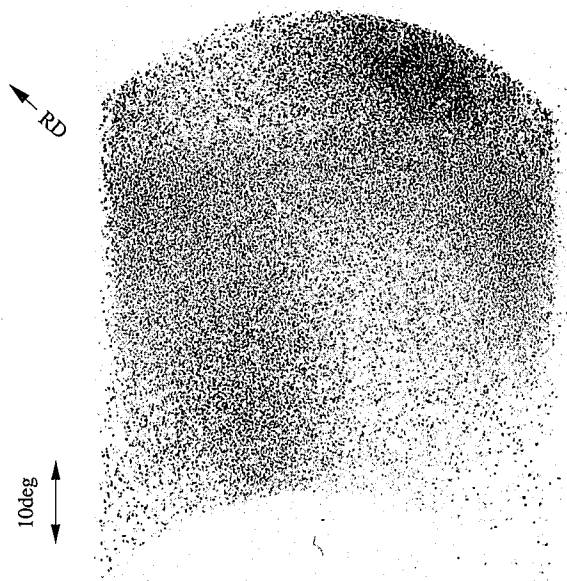


Photo 7 {100} pole figure (partial) of austenite region of Mn-Nb-Ti ultralow-carbon cold-rolled steel sheet measured by new method during isothermal holding. Sample was heated at 2 K/s, pole figure measurement was commenced 60 seconds after start of holding at 1,233 K, and projection was completed in 112 seconds. Sample rotation angle range was 56°

measured in the austenite (γ) region of steel sheets, and findings were obtained about the mechanism concerning the formation of transformation texture. Mn-Nb-Ti ultralow-carbon cold-rolled sheet steel changes little in texture and retains a good r value when it undergoes the transformation $\alpha \rightarrow \gamma \rightarrow \alpha$ after cold rolling. The mechanism involved was not clear. As shown in **Photo 7**, the authors succeeded in measuring high-temperature pole figures of the sheet steel in the austenite region for the first time in the world. They also found that variant selection increases the r value on transformation (cooling) but not reverse transformation (heating)¹³. The pole figure shown in **Photo 7** was measured for 122 seconds over a sample rotation angle range of 56°. The measurement time can be shortened to about 10 seconds.

6. Possibility of Development of New Pole Figure Method

The new pole figure method can be used to easily identify the microstructures of rolled and recrystallized metals, and it is regarded as a powerful technique for observing the primary recrystallization process of metallic materials. Besides the aluminum alloy shown in **Fig. 3** and **Photo 1**, mild steel sheets¹⁴ and stainless steel sheets¹⁵ were statically observed by the proposed method. The method allows us to observe primary recrystallized grains formed in the structure of cold-rolled materials and measuring only a few micrometers in size and to continuously observe the process after the occurrence of primary recrystallized grains. It is hoped that in the future dynamic observations at high temperatures will be successfully performed using the method. The new pole figure method can also measure pole figures, irrespective of the number of grains, and is thus suited for measuring pole figures of coarse-grained materials and microregions. It was also used to measure pole figures of coarse grains in electrical steel sheets¹⁶. A coarse-grained material can be measured even if

it contains only one grain. Minute regions of about $20 \mu\text{m} \times 20 \mu\text{m}$ can be measured, although this is related to diffraction intensity.

The high-speed and high-resolution pole figure method rapidly records in two dimensions the intensity distribution spread in the reciprocal lattice space of crystals. This involves the combination of two movements or rotation of the Ewald sphere and parallel movement of the two-dimensional detector. If the brightness of the X-ray source rises, the time interval of dynamic observation can be shortened. Given the mechanical structure of the apparatus, it is considered difficult to make the interval shorter than a period of seconds. Records taken at intervals of one to 100 seconds are expected to provide many findings about the microstructural change of materials. The new method will have increasing applications in observing the changes occurring in sheets of not only metals and alloys but also ceramics and polymers under tensile and torsional stresses, as well as thermal stresses and in magnetic fields.

Acknowledgments

The authors would like to express their sincere thanks to Dr. Yoshiyuki Amemiya of the National Laboratory for High Energy Physics' Photon Factory for advice on the use of the imaging plates, and to Dr. Satoshi Sasaki of the Tokyo Institute of Technology's Research Laboratory of Engineering Materials for advice on the optical system of the beam line BL-3A.

References

- 1) Matsuo, M.: Textures (ed. Nagashima, S.). First Edition. Maruzen, 1984, Chapter 1
- 2) Hu, H., Sperry, P.R., Beck, P.A.: Trans. AIME. 194, 76 (1952)
Kawasaki, K., Iwasaki, H.: J. Synchrotron Radiation. 2, 49 (1995)
- 3) Kawasaki, K., Iwasaki, H., Kawata, H., Nose, K.: Rev. Sci. Instrum. 63, 1110 (1992)
Kawasaki, K.: Ph.D. thesis. National Graduate University, 1992
Kawasaki, K., Iwasaki, H.: Journal of Japanese Society for Synchrotron Radiation Research. 5, 239 (1992)
- 4) Miyahara, J., Takahashi, K., Amemiya, Y., Kamiya, N., Satow, Y.: Nucl. Instr. Meth. A 246, 572 (1986)
- 5) Guinier, A.: Theorie et Technique de la Radiocristallographie. 2nd ed. Dumond, 1956, Chap. 7
- 6) Kawasaki, K., Takagi, Y., Nose, K., Morikawa, H., Yamazaki, S., Kikuchi, T., Sasaki, S.: Rev. Sci. Instrum. 63, 1023 (1992)
- 7) Sasaki, S., Mori, T., Mikuni, A., Iwasaki, H., Kawasaki, K., Takagi, Y., Nose, K.: Rev. Sci. Instrum. 63, 1047 (1992)
- 8) Taguchi, S.: Trans. ISIJ. 16, 604 (1977)
- 9) Goss, N.P.: U.S. Patent 1,965,559. 1934
- 10) MacCormack, I.B., Tanner, B.K.: J. Appl. Cryst. 11, 40 (1978)
- 11) Kawasaki, K., Matsuo, M., Ushigami, Y.: Photon Factory Activity Report. #4, 323 (1986)
- 12) Kawasaki, K., Matsuo, M., Ushigami, Y., Kawata, Y.: Tetsu-to-Hagane. 77, 204 (1991)
- 13) Yoshinaga, N., Kawasaki, K., Ushioda, K.: CAMP-ISIJ. 7, 823 (1994)
- 14) Kawasaki, K., Iwasaki, H., Yoshinaga, N.: Rev. Sci. Instrum. 66, 1404 (1995)
- 15) Shindo, T., Kawasaki, K.: CAMP-ISIJ. 8, 717 (1995)
- 16) Shimazu, T., Shiozaki, M., Kawasaki, K.: J. Mag. Mat. 133, 147 (1994)